Pergamon

Scripta Metallurgica *et* Materialia, Vol. 30, No. 11, pp.1419-1424, 1994

0956-716X/94 $6.00 + 00

$L1_2$ TO DO_{19} STRUCTURAL ORDERING DURING THE *fcc* TO *hcp* TRANSFORMATION IN A CoCrTa ALLOY

B. Cheong, Y. C. Feng and D. E. Laughlin
Department of Materials Science and Engineering
Carnegie Mellon University, Pittsburgh, PA 15213

(Received January 26, 1994)
(Revised February 15, 1994)

Introduction

In solid state phase transformations, the evolution of one state into another is realized through the motion of atoms. Such atomic motion may be either diffusional or displacive in nature. Phase transformations are often considered to involve only one type of atomic motion, but there has been mounting experimental evidence and implications about the interplay or the combination of both kinds. In principle, combined diffusional and displacive atomic motion is possible when a phase transformation involves a rearrangement of the crystal lattice as well as the reconfiguration of atoms such as decomposition or atomic ordering. Recently, we have conducted an experimental study of a phase transformation of this class (decomposition of a hyper-eutectoid CuBe alloy) and have substantiated diffusional and displacive atomic motion in conjunction with the formation of polytwin precipitate plates (1). In the present work, we examine the possibility of the transformation between the $L1_2$ and the DO_{19} phase states (ordered derivatives of *fcc* and of *hcp*, respectively) through the combination of displacive and diffusional atomic motion. The particular situation we are considering is when the stability of the $L1_2$ precipitate phase is perturbed by the shear deformation that is responsible for the transformation of the matrix *fcc* to *hcp*. To our knowledge, there has been no published work, either theoretical or experimental, on this subject. In what follows, we will first introduce experimental findings from our recent TEM study of a CoCrTa ternary alloy. We then discuss the implications of these findings by examining the transformation crystallography of the $L1_2$ ordered structure.

Experimental Procedure

Commercial Co-14.6at%Cr-2.6at%Ta alloys for sputtering targets were used in the study. The alloys were first cut into pieces about 0.5 mm thick and were reduced further in thickness to about 0.3 mm by cold-rolling. After solution treatment at 1200 °C for 4 hours, the alloys were rapidly quenched into water. The quenched alloys were annealed in a three zone Lindberg tube furnace at 750 °C for 30 hours and were then quenched into water. For each of the heat treatments, specimens were encapsulated in quartz tubes with argon gas back-filled. Overall structural states of the heat-treated alloys were examined by means of a Rigaku x-ray diffractometer equipped with a high temperature stage. To prepare the specimens for transmission electron microscopy (TEM), heat-treated alloys were reduced in thickness to about 100 μm by mechanical polishing. Discs of 3 mm in diameter were prepared and TEM specimens were made therefrom by twin-jet electro-polishing. TEM was conducted using a Phillips 420T operating at 120 kV.

Results and Discussion

Structural changes, as they occur during successive heat treatments of the CoCrTa alloy, are shown in the x-ray diffractometer profiles of Fig. 1. In Fig. 1a, taken from the alloy solution-treated and quenched in water, one can observe *hcp* peaks of sizable intensity as well as peaks due to a *fcc* phase. A TEM examination has shown that

the quenched alloy consists of two phases (*fcc* and *hcp*) of comparable volume fraction. Since the alloy is expected to be *fcc* at 1200 °C†, the *hcp* phase most likely arose from the transformation of *fcc* during the quenching process. When the alloy is annealed at 750 °C, most of the *hcp* phase transforms back into *fcc* phase. This is shown in an x-ray profile taken *in situ* from an alloy annealed for 30 hours (Fig.1b). One can observe that the *hcp* phase has almost disappeared. In light of our interest in the present study, it is not a critical issue to determine whether a small amount of *hcp* phase could exist in equilibrium at 750 °C, and no further investigation of this was attempted. When the annealed alloy is quenched in water, some of the *fcc* phase transforms into *hcp* again, as shown in Fig. 1c. The general tendency displayed here did not change for different sets of samples, except for some variation in the relative volume fractions of *fcc* and *hcp* phase in the quenched states.

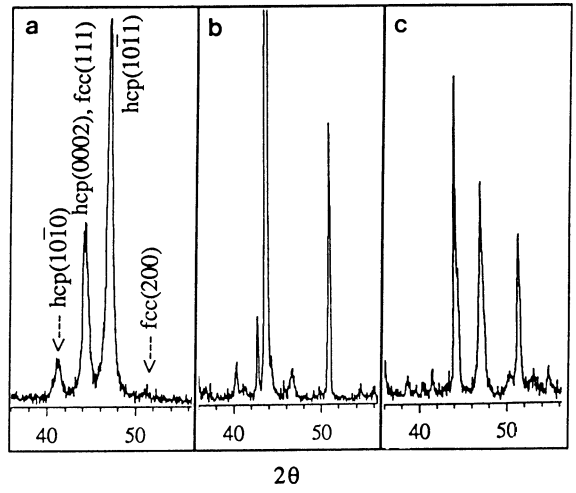

Figure 1:

X-ray diffractometer profiles of the CoCrTa alloy during successive heat treatments. (a) solution treatment at 1200 °C for 4 hours followed by water-quenching. (b) (a) + annealing at 750 °C for 30 hours (*in situ*) (c) (b) + water-quenching. Notice change in relative intensities of *fcc* and *hcp* peaks.

The aged/quenched alloys were further examined by TEM and the results are summarized in a set of TEM photographs shown in Fig. 2a to 2d. In the Bright Field (BF) micrograph (Fig. 2b), a large density of fault-like features are readily observed as well as precipitate-like contrast distributed over the entire area. The associated Selected Area Diffraction Pattern (SADP) (Fig. 2a) is analyzed and schematically reproduced in Fig. 2e. It can be seen that the microstructure consists of four phases: *fcc*, $L1_2$, *hcp* and an unknown X phase which is an ordered derivative of the *hcp* (in the schematic, the slight differences in the lattice parameters between the *fcc* and the $L1_2$ (~ 1.5 %) and between the *hcp* and the X phase are not depicted). From a Dark Field (DF) micrograph (Fig. 2c) taken with the 100 $L1_2$ superlattice reflection marked 1 in the SADP, one can see projected images of cuboidal $L1_2$ precipitates which are aligned along the $<100>_{fcc}$ directions. Inside the regions which appeared faulted in the BF image, a remarkable feature is found: thin bands of no contrast thread through the $L1_2$ precipitates along the $\{111\}_{fcc}$ traces. A DF image taken with the superlattice reflection marked 2 in the SADP, shows that the regions inside the $L1_2$ precipitates which revealed no contrast in Fig. 2c are due to X phase (notice the complementarity of the particle images from the insets of Fig. 2c and 2d). The regions of thin bands which lie outside the $L1_2$ precipitates, on the other hand, consists of the *hcp* phase, as confirmed by DF imaging using a *hcp* fundamental reflection. From this, it is apparent that X phase originates from the $L1_2$ phase, induced by the *fcc* to *hcp* transformation of the matrix.

Atomic arrangements in the close packed planes of *fcc*, *hcp* and their derivatives may be represented by a schematic diagram shown in Fig. 3. In the diagram, white, gray and black circles are used to represent three

† Equilibrium phase diagrams of both binary Co-Cr (2) and Co-Ta (3) systems show that fcc phase is stable down to temperatures well below the solution-treatment temperature employed in this study.

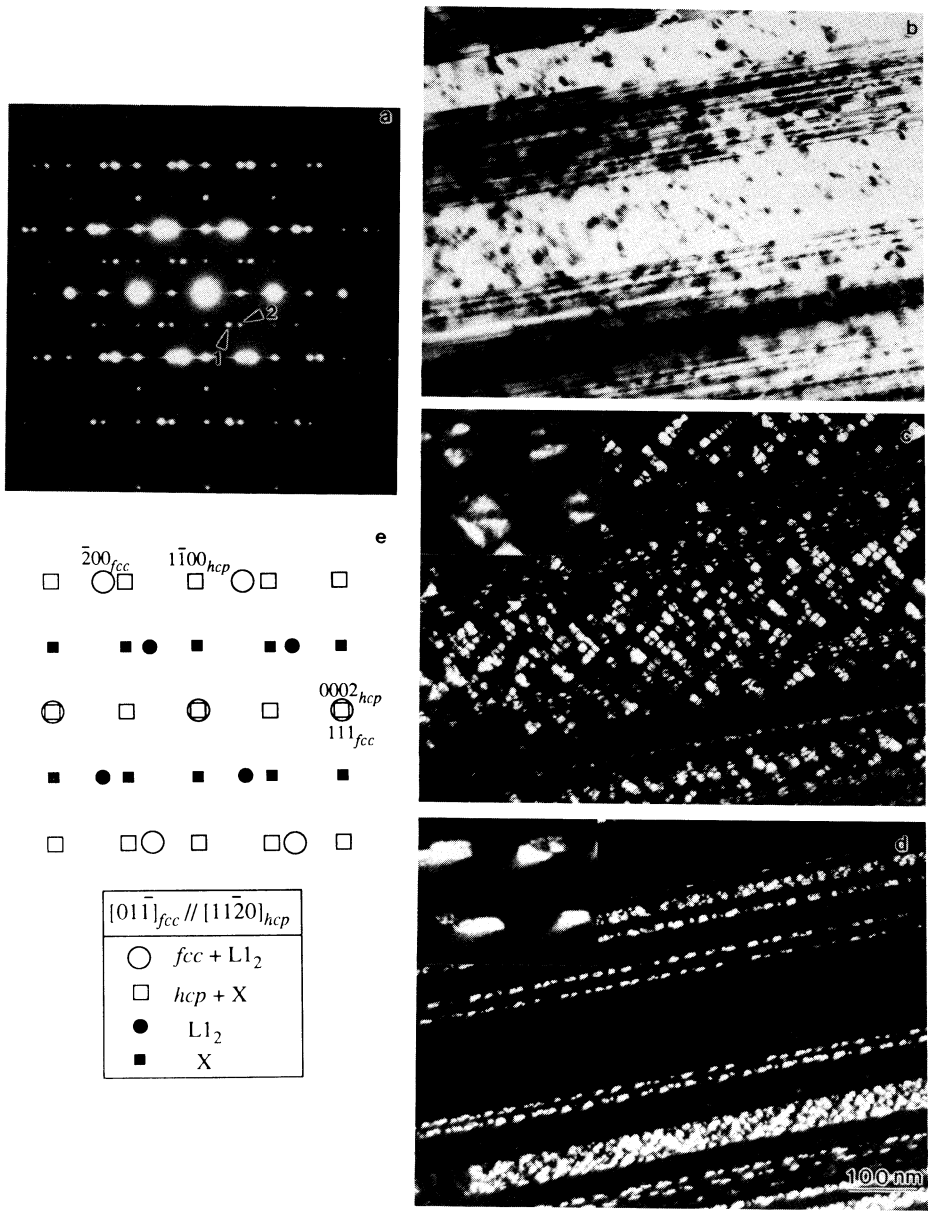

Figure 2: TEM photographs ((a) to (d)) taken from the CoCrTa alloy aged at 750 °C for 30 hours followed by water-quenching: (a) SADP, (b) BF, (c) and (d) DF images taken respectively with the superlattice reflections marked 1 and 2 in (a). A schematic of the SADP is also shown in (e). It is to be noted that some of the $L1_2$ regions are transformed to a *hcp*-derivative X phase, induced by the *fcc* to *hcp* transformation of the matrix.

different types of atomic stacking positions (commonly denoted as A, B and C) and numbers denote distinguishable individual atomic sites. In the case of a binary $L1_2$ alloy of $\alpha\beta_3$ stoichiometry, solute α atoms occupy a specific sequence of atomic sites 1-2-3-1- on successive $(111)_{fcc}$ planes: this atomic arrangement is represented A/1-B/2-C/3-A/1- in Fig. 3. Let us suppose that the $L1_2$ structure is subject to the shears which are responsible for the change of *fcc* to *hcp*. As illustrated in Fig. 3, consecutive shears by motion of Shockley partial dislocations ($a/6[\bar{2}11]$ where a is a lattice parameter) on every other (111) plane of the $L1_2$ ordered structure result in a four layer structure of a *hcp* derivative in which solute atoms occupy the atomic sites 1-2-10-5-1... on successive $(0001)_{hcp}$ planes *i.e.* A/1-B/2-A/10-B/5-A/1...

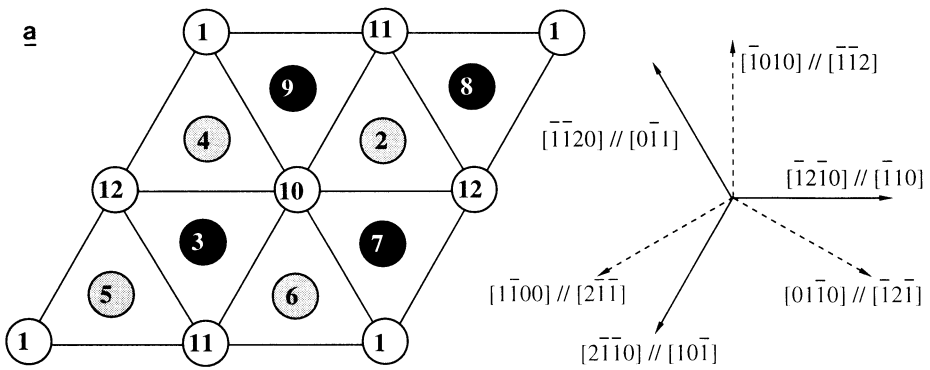

b

C / 3		A /10		B / 2		C / 8
B / 2		C / 8		A / 1		B / 5
A / 1		B / 5		C / 3	--->	A /10
C / 3		A /10		B / 2		B / 2
B / 2		C / 8	--->	A / 1		A / 1
A / 1		B / 5		B / 5		B / 5
C / 3	--->	A /10		A /10		A /10
B / 2		B / 2		B / 2		B / 2
A / 1		A / 1		A / 1		A / 1
$L1_2$		shear 1		shear 2		shear 3

Figure 3: Schematics to illustrate; (a) atomic arrangements in close packed planes of *fcc*, *hcp* and their ordered derivatives (white, gray and black circles denote atomic stacking positions of A, B and C type, respectively) and (b) change in atomic arrangement, as occasioned by dislocation motion that is responsible for the change of *fcc* to *hcp*.

It is absolutely necessary to determine whether this four layer structure could account for the observed diffraction patterns. In regard to this, one should note that the four layer structure has the 2_1-fold symmetry along the [0001] direction, instead of the hexagonal (6_3-fold) symmetry possessed by *hcp*. This renders an important guideline in diffraction study: the four layer structure would be seen different by electron beam along the [$\bar{1}\bar{1}$20] (or [1$\bar{1}$00]) direction than along [2$\bar{1}\bar{1}$0] and [$\bar{1}$2$\bar{1}$0] (or [01$\bar{1}$0] and [10$\bar{1}$0]) directions. This is illustrated in the diffraction patterns of Fig. 4 which were calculated by use of a commercial software program named Desktop Microscopist developed by Virtual Laboratories. Based on this information, a tilting experiment was conducted of the region depicted in Fig. 2. The foil normal of the region is near [11$\bar{2}$0] without tilting and consequently, both the neighboring [01$\bar{1}$0] and [10$\bar{1}$0] directions were accessible by tilting. As it turned out, diffraction patterns at both orientations displayed only the kind presented in Fig. 4a. We have also attempted extended tilting of the same

region to $[2\bar{1}\bar{1}0]$ or $[\bar{1}2\bar{1}0]$ orientation but neither zone axis was attainable. Nevertheless, it should be emphasized that the diffraction pattern shown in Fig. 4d was never observed during our TEM study so far.

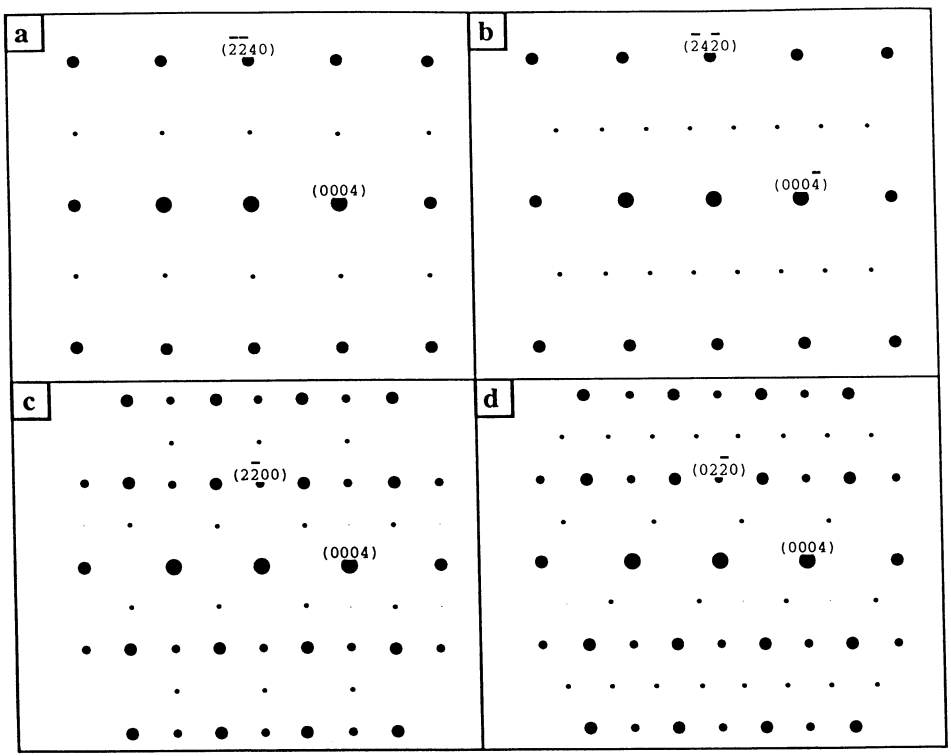

Figure 4: Calculated diffraction patterns of the four layer structure: (a) zone axis (**z**) = $[1\bar{1}00]$. (b) **z** = $[01\bar{1}0]$ or $[10\bar{1}0]$. (c) **z** = $[11\bar{2}0]$. (d) **z** = $[2\bar{1}\bar{1}0]$ or $[\bar{1}2\bar{1}0]$. The patterns c) and d) leave out the reflections due to double diffraction which would appear in actual patterns of the $<11\bar{2}0>$ type. Diffraction patterns of the kinds b) and d) have never been observed during our TEM study.

From the experimental findings, it is concluded that X phase does not have the four layer structure discussed above. We find that a probable structure that can account for all the observed diffraction patterns is the DO_{19} structure (no loss of hexagonal symmetry and thus a complete degeneracy in the $<1\bar{1}00>$ as well as in the $<11\bar{2}0>$ zone axes). As compared with the four layer structure, solute atoms in the DO_{19} structure are displaced in the 3rd and 4th layer by a unit lattice translation of the *hcp* structure, thus occupying the sites 1-2-1-2 ... on successive $(0001)_{hcp}$ planes. An interesting relationship is noticed that a domain of the four layer structure is, in effect, a domain of the DO_{19} structure with periodic APB's. This close structural relationship is generic in the sense that any structure accountable for X phase should derive from the four layer structure, since the initial formation of the four layer structure is enforced by the concurrent *fcc* to *hcp* transformation.

There are two important questions regarding the formation of the DO_{19} structure. The first question is whether the DO_{19} structure is favored energetically over the four layer structure. With regard to this, it should be noted that configurational characteristics of atomic bonding in the DO_{19} structure are quite similar to those in the $L1_2$ structure. To be specific, every solute atom in both the structures (of $\alpha\beta_3$ stoichiometry), is surrounded

completely by solvent atoms in the first nearest neighbor shell, whereas a solute atom has a nearest neighbor atom of its own kind in the four layer structure (Carnahan *et al.* first discussed this aspect with respect to the stacking faults in the $L1_2$ ordered structure (4)). In view of the fact that the untransformed $L1_2$ precipitates are most likely enriched by Ta atoms (Co_3Ta base (3)) and that Ta atoms are larger than Co and Cr atoms which are comparable in size, the presence of a solute-solute (*i.e.* Ta-Ta) nearest neighbor pair in the bonding environment upheld in either $L1_2$ or DO_{19} structure, is particularly an unfavorable feature that would lead to increase in internal energy. Accordingly, we consider that the four layer structure is not stable with respect to transition to the DO_{19} structure.

The other question that attaches more interest to the present experimental results is concerned with the atomic mechanism of the formation of the DO_{19} structure, that is, of the change in solute atom stacking sequence from 1-2-10-5.. to 1-2-1-2... We do not believe that this additional arrangement of atoms actually occurs by motion of unit translation dislocations (of either *hcp* or *fcc*) on every other close packed plane. There appears to be no physical source of such periodic displacive atomic motion, since it is not demanded by and thus can not originate from the concurrent *fcc* to *hcp* transformation. Neither is there any reasonable ground to suppose that the prescribed dislocation motion occurs selectively in the precipitate region. This leaves the other mechanism as a strong possibility, that is, diffusional motion of atoms.†† It is not readily understood how the rearrangement of atoms, best described as simultaneous translation of collective atoms, could be achieved by individual atomic diffusion, however, and this is to be resolved in future studies. We speculate that such diffusional atomic rearrangement might occur with the passage of a Shockley partial dislocation, that is, along the moving interface between the $L1_2$ and the DO_{19} phase.

Conclusions

We have presented experimental findings which show an interesting phase change that is undergone by the $L1_2$ precipitates during the *fcc* to *hcp* transformation in the matrix of the CoCrTa alloy. From consideration of the transformation crystallography and from detailed diffraction pattern analyses, we have shown that the resulting phase has the DO_{19} structure, not the four layer structure that derives directly from the $L1_2$ structure by shear deformation responsible for *fcc* to *hcp* transformation. Under the given circumstance, the formation of the DO_{19} structure seems to involve diffusional atomic motion subsequent to the enforced displacive motion of atoms.

Ackonwledgements

The authors wish to thank Mr. Jason Wolf for providing technical assistance in acquiring hot-stage x-ray data. This work was supported by Department of Energy under the grant DE-FG02-90-ER45423.

References

1. B. Cheong, K. Hono and D. E. Laughlin, *Met. Trans.*, **24A**, 2605 (1993); *Acta metall. mater.*, in press.
2. K. Ishida and T. Nishizawa, *Bull. Alloy Phase Diagrams*, **11**, 357 (1990).
3. R. D. Dragsdorf and W. D. Forgeng, *Acta Cryst.*, **15**, 531 (1962).
4. T. Carnahan, B. Cullen, J. Demel, J. Mcllwain, M. J. Marcinkowski, J. Munford, J. Pahlman, T. Prevender and J. Warner, *TMS-AIME*, **239**, 2014 (1967).

†† Regarding this possibility, one might think of another possible crystal structure in which atomic sites of solute atoms may be represented as 1-2-random-random.. This structure does not render the observed diffraction patterns, however.